Optical Demonstration of a Crystal Band Structure Formation

M. Bayer, T. Gutbrod, and A. Forchel
Technische Physik, Universität Würzburg, Am Hubland, D-97074 Würzburg, Germany

T. L. Reinecke
Naval Research Laboratory, Washington, D.C. 20375

P. A. Knipp
Christopher Newport University, Newport News, Virginia 23606

R. Werner and J. P. Reithmaier
Technische Physik, Universität Würzburg, Am Hubland, D-97074 Würzburg, Germany
(Received 1 June 1999)

The optical modes of chains of coupled micron sized semiconductor cavities have been studied using photoluminescence spectroscopy and detailed calculations. With an increasing number of cavities, the chains exhibit photon band gaps at several Brillouin zone boundaries. The sizes of the band gaps are shown to depend on the coupling between the microcavities and also on the order of the Brillouin zone involved.

PACS numbers: 78.55.Cr, 42.70.Qs

Systems which exhibit photon band gaps analogous to the band gaps in the electronic states of periodic solids have been the subject of intense investigations in the past decade [1–3]. In the photonic case, the forbidden energy gaps in the frequency spectrum result from a periodic modulation of the refractive index. These systems are called "photonic crystals" and calculations of their properties for a number of structures have been made [1,2,4]. They permit the coupling between photons and electronic excitations to be studied and controlled in powerful ways, including the introduction of highly localized defect modes in the band gaps.

Experimentally, to date photonic crystals have been realized over several parts of the electromagnetic spectrum [5–14]. The near infrared and the visible range is particularly important for potential applications as well as for fundamental studies [15,16]. Photonic crystals could be used, for example, to obtain semiconductor lasers with zero, or low, threshold due to the possibility of suppressing the spontaneous emission by photonic energy gaps. Defect modes in band gaps are of interest in connection with waveguides for ultrasmall integration.

Recently it has been shown that micron sized semiconductor resonator cavities exhibit sharp photonic resonances resulting from the strong optical confinement in all three directions [17–19]. The vertical confinement of the photon modes is effected by Bragg mirrors, and the lateral confinement is caused by etching of the cavity. In this way, strong photonic resonances are created in the cavities whose energies are controlled by the cavity size. These modes are analogous to the sharp electronic states of atoms or quantum dots.

In the present work we have created a photonic band gap system for frequencies in the near infrared by putting together microcavities in chains. We are able to construct a system by adding individual building blocks ("photonic atoms") one by one. Angle-resolved photoluminescence spectroscopy is used to study the emergence of a photonic band structure: In chains formed from an increasing number of cavities we observe a transition from discrete atomiclike modes to the photonic band structure of a solid with band gaps at several Brillouin zone boundaries. We are able to modify the modulation of the refractive index by varying the coupling between the cavities, and the energy gaps are found to increase with increasing modulation. We show that the experimental results are in quantitative agreement with numerical calculations of the photonic band structure made for these systems.

The photonic chains were fabricated by lithographic patterning of planar semiconductor microcavities. An $In_{0.10}Ga_{0.90}As$ quantum well forms the optically active material in the center of a GaAs cavity surrounded by Bragg mirrors. A description of these structures has been given elsewhere [20]. Figure 1 shows a scanning electron micrograph of sections of linear chains each made of 50 coupled cavities in total. The size of each cavity is $3 \times 3\ \mu m^2$. Each cavity is coupled to its neighbors by a narrow channel of width W and length L ($W = 1.5\ \mu m$ and $L = 1\ \mu m$ in Fig. 1). This system is similar to the two dimensional photonic crystal operating in the microwave range studied by Sievenpiper *et al.* [9] We are able to vary the periodic modulation of the refractive index along the chains by varying the lengths or widths of the channels connecting the cavities. In the present work we vary between weak modulation for $W = 2.5\ \mu m$ and strong modulation with $W = 1.5\ \mu m$.

The optical modes in the chains have been studied by angle-resolved photoluminescence spectroscopy:

 0031-9007/99/83(25)/5374(4)$15.00

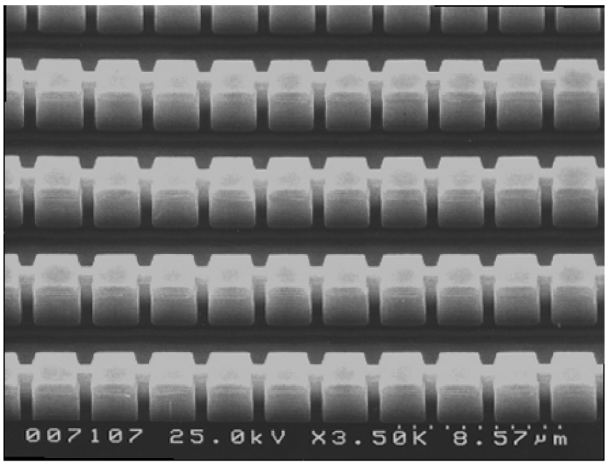

FIG. 1. Scanning electron micrograph of sections of photonic chains each made from 50 coupled cavities described in the text. The channels connecting the cavities have length $L = 1\ \mu$m and width $W = 1.5\ \mu$m.

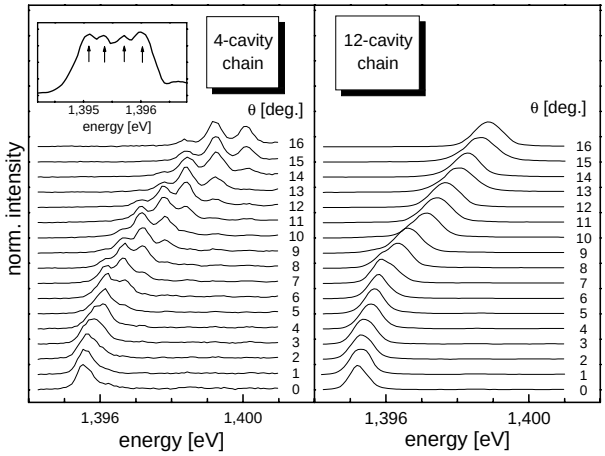

FIG. 2. Angle-resolved photoluminescence spectra of the chains formed from 4 cavities (left) and 12 cavities (right) for increasing angle of observation along the chains (channel $L = 1\ \mu$m and $W = 2.5\ \mu$m). The inset in the left panel gives an angle integrated spectrum recorded with a high resolution of the ground photon feature.

The samples were held at $T = 5$ K in an optical cryostat, and an Ar-ion laser ($\lambda = 514.5$ nm) was used to excite electron-hole pairs at low excitation powers ($0.1\ \mathrm{W\,cm^{-2}}$). After photoexcitation the carriers relax into the quantum well whose ground state exciton at 1.420 eV is separated far from the low lying photon branches of interest here. Thus the exciton polariton branches are weakly coupled. The emission of the photonlike branches was detected in a small aperture. The aperture could be moved parallel to the cavity plane, so that the direction of detection could be varied in the plane given by the normal to the cavity and the chain axis. This direction is characterized by the angle ϑ relative to the cavity normal. The diameter of the aperture was adjusted for providing an angular resolution of 1°. The luminescence was dispersed by a double monochromator ($f = 1$ m) and detected by a photomultiplier interfaced with a photon counting system.

Figure 2 shows photoluminescence spectra recorded for varying angles of detection along chains of 4 and 12 cavities. In this case the lengths and widths of the connecting channels were 1 and 2.5 μm, respectively giving a weak modulation of the refractive index. The spectra obtained for an angle variation between $\vartheta = 0°$ (normal to the surface) and 16° show striking changes for these two chains. The spectra of the 4-cavity chain have a set of discrete modes. For increasing angles, modes at higher energies dominate the spectra, and low energy modes vanish. However, the energy of a given mode is independent of the angle of detection, except for the ground mode, which seems to disperse to higher energies. The angle-integrated high resolution spectrum in the inset of Fig. 2 shows that this low energy feature consists of four discrete molecular modes which have constant energies for varying ϑ. This behavior is a signature of fully confined photon modes.

For the 12-cavity chain, in contrast, the emission is characterized by a single line, which appears to shift continuously to higher energies with increasing angle. Neglecting the weak refractive index modulation, the transition energies of the longer chain can be understood qualitatively by considering a long wire with constant width. Its transition energies are given by $E = (E_0^2 + E_y^2 + \hbar^2 c^2 k_x^2)^{1/2}$, where E_0 is the energy of the fundamental mode of the planar cavity and E_y is the optical confinement energy perpendicular to the chain [21]. k_x is the photon wave vector along the chain, which is related to ϑ by $k_x = \sin\vartheta E/(\hbar c)$.

Figure 3 shows the optical mode peak energies versus the angle of detection for chains made from varying numbers of cavities. The lengths and widths of the channels are the same 1 and 2.5 μm as in Fig. 2. The energies in the 2-cavity chain do not depend on ϑ. In this case the electromagnetic fields are three dimensionally confined as in the case of single cavities. The modes in the 4-cavity chain also have cavitylike character, but the energy splitting between the confined modes is reduced due to the larger chain length. For 8 coupled cavities a further reduction of the mode energy splitting is observed as well as an apparent shift of the modes to higher energies with increasing ϑ. Finally, for 12 coupled cavities a discrete optical mode spectrum can no longer be resolved, and the modes form a continuum with dispersion along the chain. No apparent changes are observed when the number of coupled cavities is increased above 12.

We have generated an interpretation of the transformation seen between small numbers of cavities and large numbers in Fig. 3 based on detailed calculations for these structures. For small numbers of cavities, the modes form groups with closely spaced levels with the energy of each

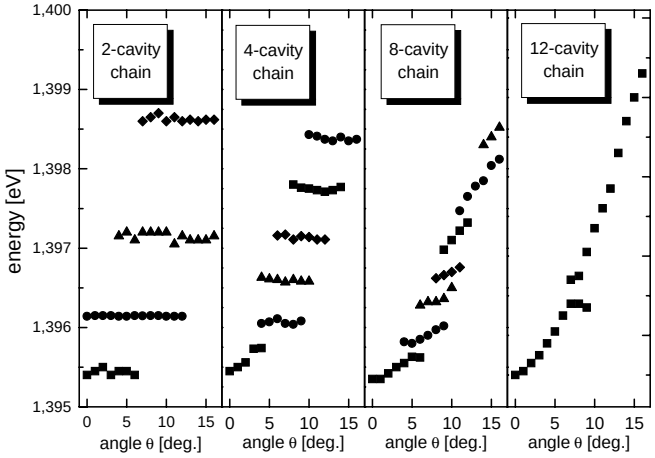

FIG. 3. Energies of optical modes versus the angle ϑ along the chains for varying numbers of coupled cavities (channel $L = 1\ \mu$m and $W = 2.5\ \mu$m).

group determined by confinement perpendicular to the chain and with the energies within the group resulting from confinement along the chain. Within each group, the calculated maxima of the emission intensity move to a higher angle as the energy of the mode increases. It is these intensity maxima which are observed, giving rise to the onset of apparent dispersion. For the 12-cavity chain, these intensity maxima move through a closely spaced, near continuum of states, which becomes a continuum as the number becomes infinite.

With the channel length and width of the structures in Figs. 2 and 3 the dielectric function is rather weakly modulated. However, even this weak modulation causes deviations from a photonic wirelike behavior, as seen for the 12-cavity chain in Fig. 2. Around $\vartheta = 7°$ the emission line does not shift continuously to higher energies, but two lines are observed with an energy separation of about 0.2 meV.

To obtain further insight into the influence of a periodic modulation of the refractive index on the dispersion, long chains with a larger index modulation have been studied. Figure 4 shows angle-resolved spectra of a chain made from 50 coupled cavities with a channel length of 1 μm and a width of 1.5 μm. For increasing angles below 6° the optical mode shifts slightly to higher energies. Around 7° a second mode appears at about 1.3 meV higher energy. For angles up to 15° this mode becomes the dominant one. At about 14° to 15° another mode appears at 1 meV higher energy. This mode dominates the spectra up to an angle of 28°. Then a further mode appears at higher energy.

Figure 5 shows the energies of the photon mode emissions versus the wave vector k_x along the chain for a 50-cavity chain. For comparison the photon mode dispersion in a 3 μm wide wire without modulation also is shown (dash-dotted line). Three discontinuities are observed in the dispersion for the modulated chain. At these features there are strong deviations from the

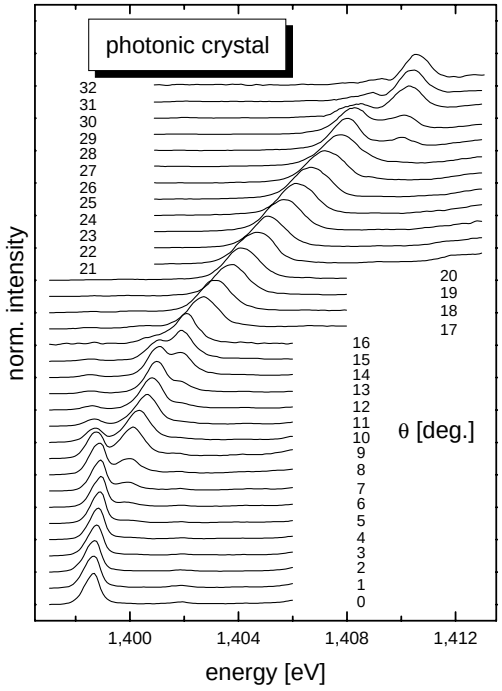

FIG. 4. Angle-resolved photoluminescence spectra of a chain of microcavities for varying angle along the chain (channel $L = 1\ \mu$m and $W = 1.5\ \mu$m).

dispersion of a wire of constant width resulting in gaps in the frequency spectrum of ~1.3, 0.8, and 2.1 meV.

Energy gaps in periodically modulated structures can occur at the boundaries of the Brillouin zones, which are located at $k_{\mathrm{BZ}} = n\pi/P, n = \pm 1, 2, \ldots$, with the lattice constant P and the zone number n. The dotted vertical lines in Fig. 5 indicate these zone boundaries. The discontinuities observed in the spectra in Fig. 4 correspond to energy gaps at the boundaries of the first, the second, and the fourth zones. At the boundary of the third Brillouin zone, surprisingly, no energy gap is found in the experiment.

Detailed numerical calculations using the boundary element method [22] of the photonic dispersions in these chains have been made and are shown by the solid lines in Fig. 5. We observe good agreement with experiment for all parts of the photonic band structure. In particular, at the third zone boundary the calculated gap is 0.035 meV, which is too small to be resolved in the experiment. This small gap arises from the small third Fourier component of the periodically varying refractive index in the present structures.

The size of the band gaps is determined by the strength of the modulation of the effective crystal potential. For photons, this modulation is given by the variation of the dielectric function along the chain, and it can be modified by changing the width of the channels. The inset in Fig. 5 shows the gaps at the first zone boundary versus the channel width for chains with a channel length of 1 μm.

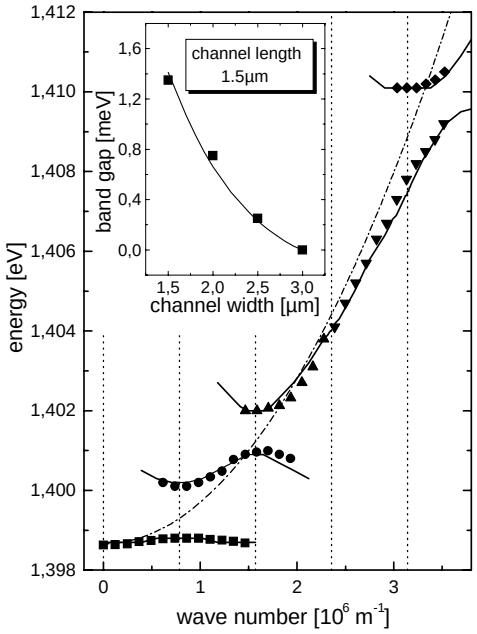

FIG. 5. Energy dispersion in a chain (channel $L = 1$ μm and $W = 1.5$ μm). Symbols give the experimental data; the solid lines give the results of the calculations. The dash-dotted line gives the dispersion in an unmodulated photonic wire. Vertical lines give Brillouin zone boundaries. The inset shows the dependence of the energy gap at the first zone boundary on the channel width.

For a channel width of 3 μm the structure becomes a photonic wire and no band gap is observed. With decreasing channel width the modulation of the dielectric function increases, and larger band gaps are observed in agreement with the calculations (solid lines).

In summary, we have used coupled semiconductor microcavities as building blocks for chains which are shown to exhibit the band gaps of a photonic crystal. This work provides a novel implementation of a photonic band gap system for optical frequencies in which we have been able to study the transition between discrete atomlike photon modes and the quasicontinuous dispersion of a photonic crystal.

This work was supported by the State of Bavaria, the Deutsche Forschungsgemeinschaft, and the U.S. Office of Naval Research.

[1] E. Yablonovitch, Phys. Rev. Lett. **58**, 2059 (1987).
[2] S. John, Phys. Rev. Lett. **58**, 2486 (1987).
[3] See, for example, J. D. Joannopoulos, P. R. Villeneuve, and S. Fan, *Photonic Crystals, Molding the Flow of Light* (Princeton University Press, Princeton, NJ, 1995); J. D. Joannopoulos, P. R. Villeneuve, and S. Fan, Nature (London) **386**, 143 (1997).
[4] K. M. Ho *et al.,* Phys. Rev. Lett. **65**, 3152 (1990); S. Satpathy *et al., ibid.* **64**, 1239 (1990); Z. Zhang *et al., ibid.* **65**, 2650 (1990); K. M. Leung *et al., ibid.* **65**, 2646 (1990); E. Yablonovitch *et al., ibid.* **67**, 2295 (1991); J. B. Pendry *et al.,* Phys. Rev. Lett. **69**, 2772 (1992).
[5] E. Yablonovitch *et al.,* Phys. Rev. Lett. **67**, 2295 (1991).
[6] E. Yablonovitch *et al.,* Phys. Rev. Lett. **67**, 3380 (1991).
[7] S. L. McCall *et al.,* Phys. Rev. Lett. **67**, 2017 (1991).
[8] W. M. Robertson *et al.,* Phys. Rev. Lett. **68**, 2023 (1992).
[9] D. F. Sievenpiper *et al.,* Appl. Opt. **37**, 2074 (1998).
[10] P. L. Gourley, Nature (London) **371**, 571 (1994).
[11] T. Krauss *et al.,* Nature (London) **383**, 699 (1996).
[12] J. S. Foresi *et al.,* Nature (London) **390**, 143 (1997); P. R. Villeneuve *et al.,* Phys. Rev. B **54**, 7837 (1996).
[13] D. Labilloy *et al.,* Phys. Rev. Lett. **79**, 4147 (1997).
[14] O. Painter *et al.,* Science **284**, 1819 (1999).
[15] S. Fan *et al.,* Phys. Rev. Lett. **78**, 3294 (1997).
[16] A. Mekis *et al.,* Phys. Rev. Lett. **77**, 3787 (1996).
[17] J. M. Gérard *et al.,* Appl. Phys. Lett. **69**, 449 (1996); Phys. Rev. Lett. **81**, 1110 (1998).
[18] J. P. Reithmaier *et al.,* Phys. Rev. Lett. **78**, 378 (1997).
[19] M. Bayer *et al.,* Phys. Rev. Lett. **81**, 2582 (1998).
[20] T. Gutbrod *et al.,* Phys. Rev. B **57**, 9950 (1998).
[21] A. Kuther *et al.,* Phys. Rev. B **58**, 15 744 (1998).
[22] P. A. Knipp *et al.,* Physica (Amsterdam) **2E**, 920 (1998).